Geophys. J. Int. (2004) **157,** 1007–1016 doi: 10.1111/j.1365-246X.2004.02228.x

Angular dependence of the switching field and implications for gyromagnetic remanent magnetization in three-axis alternating-field demagnetization

Karen Nørgaard Madsen

Institute of Solid Earth Physics, Allégaten 41, N-5007 *Bergen, Norway. E-mail: dkkms@coloplast.com*

Accepted 2003 December 19. Received 2003 July 15; in original form 2002 February 13

SUMMARY

The critical field for reversing the magnetic moment of a single-domain (SD) grain, the switching field, is a function of the angle between the field and the grain's easy axis of magnetization. The functional relationship derived for coherent reversal, i.e. spins reversing in unison, differs from that of various incoherent mechanisms and of domain wall movement in multidomain (MD) grains. Due to the angular dependence of the switching field, uniaxial alternating-field (AF) demagnetization is less efficient than AF demagnetization with tumbling of the sample. The difference was determined for synthetic and natural rock samples carrying anhysteretic and rotational remanent magnetizations (ARM and RRM respectively). These types of remanence were chosen to activate dominantly SD grains, and their magnitudes relative to saturation isothermal remanent magnetization (SIRM) are discussed in relation to magnetic grain size. For the samples studied, data indicated that the majority of remanence carriers cannot be associated with the Stoner–Wohlfarth model for coherent reversal. In contrast, incoherent reversal or domain wall movement largely explains the observed lag. Based on the angular dependence of switching field corresponding to these models, the acquisition of gyromagnetic remanent magnetization (GRM) during three-axis demagnetization is discussed. In particular it is shown theoretically that the method of Dankers and Zijderveld fails to eliminate completely the effect of GRM in three-axis demagnetization.

Key words: alternating field demagnetization, angular dependence, ARM/SIRM ratio, gyromagnetic remanence, single-domain grain, switching field.

INTRODUCTION

The most stable natural remanent magnetization (NRM) of rocks is accepted to be carried by single-domain (SD) grains of magnetic minerals and the theory of rock magnetism has focused extensively on this type of grain. The high stability of remanence carried by SD grains is attributed to the existence of strongly preferred directions of magnetization due to crystalline and/or shape anisotropy of the grain. To switch the remanent magnetization of the grain from one energy minimum state to another requires the application of a minimum field, the switching field H_r, which is typically several orders of magnitude stronger than the geomagnetic field. Magnetization processes have usually been treated based on Stoner–Wohlfarth theory (Stoner & Wohlfarth 1948) for coherent reversal, i.e. rotation in unison of the atomic spins. However, newer theoretical models indicate that coherent reversal is the preferred switching mode only for very small or nearly spherical magnetic grains close to or below the superparamagnetic threshold (Moon & Merrill 1988; Enkin & Williams 1994). For larger or more elongated grains, incoherent modes, of which several have been proposed (see e.g. Jacobs & Bean 1955; Frei *et al.* 1957), are energetically favoured.

Apart from lowering the switching field, incoherent switching modes also give rise to a different dependence of H_r on the angle θ between the field and the grain's easy axis of magnetization (Fig. 1). Unless samples are tumbled during alternating-field (AF) demagnetization, this angular dependence will influence the results. The different demagnetization behaviour can be utilized to obtain experimental evidence for coherent or incoherent switching of SD grains. McFadden (1981) calculated demagnetization curves of isothermal remanent magnetization (IRM) for two models, one assuming coherent reversal of SD grains the other modelling for domain wall movement in multidomain (MD) grains under the assumption that the effective demagnetizing field is the component parallel to the easy demagnetization axis of the grain. Mathematically the latter model was treated as equivalent to assuming $H_r(\theta) \propto 1/\cos\theta$, which is also the type of angular dependence associated with incoherent reversal of SD grains. A rough comparison with data demonstrated that this model provided a better description (McFadden 1981) than

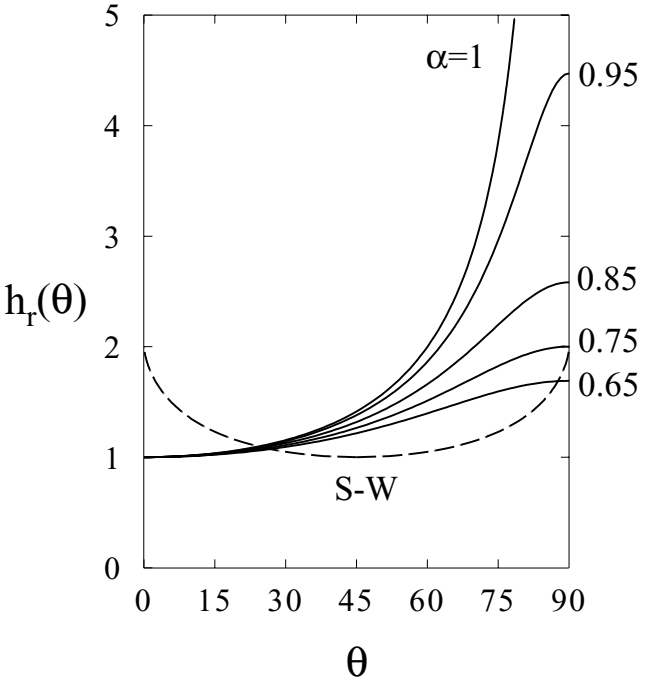

Figure 1. Switching field h_r as a function of angle θ between the field and the grain's easy axis of magnetization, normalized to make the minimum switching field $h_r = 1$. The dashed curve marked S–W is the Stoner & Wohlfarth (1948) relation for coherent reversal. For the incoherent reversal modes, switching is most readily achieved with the field applied at low angles to the easy axis of magnetization. For higher angles the switching field increases, first slowly then more rapidly. This behaviour may be parametrized by curves of $(1 - \alpha \sin^2\theta)^{-1/2}$ as suggested by Aharoni (1986). Different values of the parameter α (used to label the curves) apply to particles of different material, size and shape.

that of coherent reversal. Since MD particles as well as SD particles contribute to IRM, this result is likely to reflect the dominance of domain wall movement in MD grains rather than incoherent switching of SD grains.

The present study attempts a more quantitative comparison of model predictions and data from a demagnetization experiment. To suppress remanence contributions from MD grains, anhysteretic and rotational remanent magnetization (ARM and RRM) rather than IRM were studied. For natural samples with a mixed domain state the magnetic hardness of ARM and RRM is generally higher than that of IRM and for this reason SD grains are believed to constitute a more dominant group of remanence carriers. ARM is often used as a laboratory analogue for thermomagnetic remanent magnetization (TRM). RRM is also a remanence of practical relevance, being one type of gyromagnetic remanent magnetization (GRM), which may also be induced during static AF demagnetization. The angular dependence of switching field has implications for laboratory methods where samples are exposed to non-saturating fields. In this study GRM formation during static three-axis demagnetization is considered based on the conclusions concerning RRM carriers. In particular a method proposed to eliminate the contribution from GRM to demagnetization data (Dankers & Zijderveld 1981) is evaluated from a theoretical point of view. GRM correction in three-axis AF demagnetization has been reported to fail (Hu *et al.* 1998) and the angular dependence of the switching field offers a possible explanation.

METHOD

Numerous experiments can be designed to highlight the different angular behaviour of coherent and incoherent reversal mechanisms. The approach taken in this study requires two different kinds of stepwise AF demagnetization of each laboratory-induced remanent magnetization. Tumbling of the sample, as employed in the first demagnetization, presents all grains at essentially all angles to the field. Thus from the demagnetization curve the spectrum of coercivities is obtained, defining the coercivity H_c of a grain to be the minimum switching field, i.e. for incoherent reversal $H_c = H_r(0)$, whereas for coherent reversal $H_c = H_r(45^\circ)$. Subsequent static uniaxial demagnetization with the AF applied along the axis of the reinduced remanence brings out the angular dependence of the switching field. Knowing the distribution of coercivities from the demagnetization with tumbling, predictions for the uniaxial demagnetization are calculated assuming various models for $H_r(\theta)$ and compared with data.

RRM was induced with the sample rotating in an a 50 Hz AF of peak field strength 95 mT, the axis of rotation being perpendicular to the field axis. The rotation speed was approximately 90 revolutions per second (rps), and the ambient field was reduced to less than 0.1 μT using a Helmholtz configuration. To activate the same grains by RRM and ARM acquisition, a rotational ARM (hereafter referred to simply as ARM) was induced with the same AF and rotation axis as in the case of RRM and a biasing direct field $B_a = 150$ μT applied parallel to the rotation axis. The rotation rate during ARM acquisition was 17–18 rps, for which RRM is small for magnetite (Potter & Stephenson 1986) as well as for recording particles of CrO_2 and γ-Fe_2O_3 (Madsen 2003). A test with the biasing field off demonstrated that the contribution from RRM to this remanence was indeed negligible for all samples. In addition to ARM and RRM, the magnitude of saturation isothermal remanent magnetization (SIRM) induced in a field of about 4 T, delivered by a pulse magnetizer, was measured for all samples. For two synthetic samples the demagnetization experiment was also carried out on the SIRM.

Stepwise demagnetization with two-axis tumbling was carried out in peak fields up to 60 mT, which was the maximum field available for the tumble demagnetizer. For the uniaxial demagnetization a 2 G demagnetizer was used, for which the field values were calibrated to those of the tumble demagnetizer. The final field strength used in uniaxial demagnetization was somewhat less than that of tumbling, so a final tumbling in a peak AF of 60 mT served to check that not only the starting remanence but also the remanence remaining after demagnetization with tumbling in a peak AF of 60 mT was similar in the two runs. For some samples the intensity of demagnetized remanence varied by a few per cent between the two demagnetization runs, but for most samples the variation was less than 1 per cent.

CALCULATION OF DEMAGNETIZATION CURVES

For a sample containing magnetic grains with a spectrum of coercivities, the intensity of remanence may be expressed as a sum of contributions from grains belonging to different coercivity intervals. Let $I_{H_c}(H)$ denote, for a single coercivity H_c, the relative intensity remaining after AF demagnetization in peak field H, i.e. $I_{H_c}(H)$ is the demagnetization curve for grains of coercivity H_c only, normalized to make the initial intensity equal to unity. The intensity of the

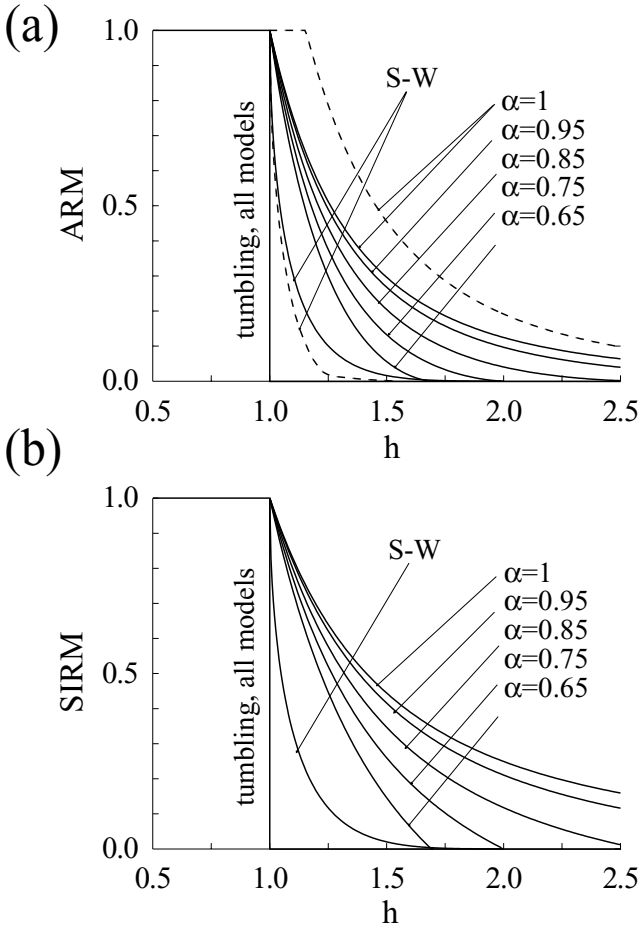

Figure 2. Calculated uniaxial demagnetization curves $I_{H_c}(H)$ of (a) ARM and (b) SIRM for an isotropic single-coercivity sample. Full lines are used for the case of saturated initial remanence. Dashed lines illustrate the effect when the magnetizing field is not saturating. In case of coherent reversal, demagnetization of a non-saturated ARM is completed at lower fields than required to demagnetize the saturated remanence. For incoherent reversal, a non-saturated ARM demagnetizes less readily than a saturated ARM. See text and Fig. 3 for discussion.

sample after demagnetization in peak field H is the sum over the intensity remaining in each coercivity interval:

$$I(H) = \sum_{H_c} I_{H_c}(H)\rho(H_c)\Delta H_c, \tag{1}$$

where $\rho(H_c)\Delta H_c$ is the relative contribution to remanence from grains of coercivities in a small interval ΔH_c around H_c. The coercivity distribution $\rho(H_c)$ is known from the demagnetization with tumbling. The intensity decrease $I_{H_c}(H)$ as a function of peak field H for an isotropic distribution of identical grains of coercivity H_c is derived in the appendix and the results are displayed in Fig. 2. The calculations were carried out for two different models of $H_r(\theta)$. One is the Stoner–Wohlfarth curve derived for coherent reversal (Fig. 1), the other is the class of curves given by

$$\frac{H_r(\theta)}{H_r(0)} = \frac{1}{\sqrt{1-\alpha\sin^2\theta}}, \qquad 0 \le \alpha \le 1, \tag{2}$$

which have been suggested based on theoretical derivations to describe incoherent switching for elongated particles of various size and shape (Aharoni 1986). For $\alpha = 1$ the right-hand side of eq. (2) reduces to $1/\cos\theta$.

In addition to the angular dependence assumed to describe the switching field of the grains, the demagnetization curves also depend on the type of remanence induced in the sample. For SIRM the contribution of each grain is taken as proportional to cos ω, ω being the angle between grain magnetic moment and the axis of sample remanence (The angles θ and ω are identical for SIRM, whereas for rotational ARM and RRM, $\omega = \frac{\pi}{2} - \theta$ (see Fig. 3).

Contributions from individual grains to ARM are taken as proportional to $\cos^2\omega$ due to the projection of the biasing field on the grain's easy axis of magnetization (Stephenson 1983). As a result of the stronger enhancement of ARM for small ω, the initial decrease of ARM during demagnetization is larger than for SIRM (Fig. 2). Considering RRM, Stephenson & Potter (1987) found that $B_g = B_a \times RRM/ARM$ determined for anisotropic samples of γ-Fe_2O_3 recording particles was independent of the degree of uniaxial particle alignment but seemed slightly dependent on the rotation axis for which it was determined, being smaller for the axis of alignment than for axes perpendicular to the alignment axis. From the lack of dependence on anisotropy it may be inferred that the relative contributions to remanence from grains with low and high ω must be the same for RRM and ARM. The dependence on the axis for which B_g is determined seems to contradict this conclusion, implying that RRM acquisition is less enhanced for small ω than is the case for ARM. The authors themselves raised doubts about the latter result, and for the present purpose it will be accepted as a working hypothesis that the demagnetization curve derived for ARM applies to RRM as well.

The ARM and RRM of the experiment were induced in a peak AF of 95 mT and thus cannot be considered saturated for the highest coercivities studied (~60 mT), since the field needed to switch the remanence of unfavourably orientated grains is typically at least double the minimum switching field (Fig. 1). Hence, calculation of the demagnetization curve begins with a calculation of the initial magnetization. For incoherent reversal the grains favourably oriented for magnetization with the field in the x–y plane are unfavourably oriented for demagnetization with the field applied along the z-axis (Fig. 3), whereas for coherent reversal the dominant contributors to remanence that are favourably oriented for magnetization are also favourably oriented for demagnetization. For this reason an unsaturated ARM will demagnetize less readily than a saturated ARM in the incoherent case and more readily in the coherent case (Fig. 2).

SAMPLES AND DATA

The samples used for the experiment are listed in Table 1. Two samples (SR8 and CK4013) were prepared from γ-Fe_2O_3 and CrO_2 recording particles by setting 0.5 and 50 mg respectively of the magnetic powders in a resin to make cylindrical samples of volume 6 cm^3. According to the manufacturer's data the recording particles are strongly elongated, their length to width ratio being 1:5 with a particle length 0.5 μm for γ-Fe_2O_3. The CrO_2 particles are of similar shape, but about half the length. In spite of thorough stirring and other care taken during preparation of the synthetic samples, it is most likely that some clustering of the magnetic particles is present and thus that magnetic interactions have a greater influence than expected if the particles had been perfectly distributed in the resin.

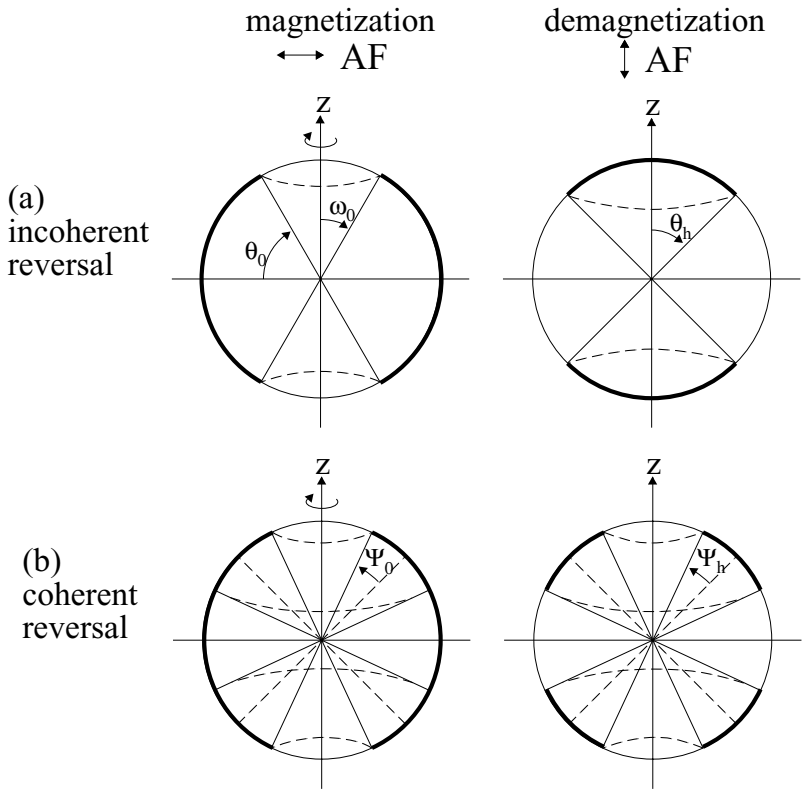

Figure 3. Sketch illustrating (left) acquisition of RRM or rotational ARM when the peak AF is non-saturating and (right) demagnetization the in case of (a) incoherent reversal and (b) coherent reversal. Magnetization is achieved with the AF applied perpendicular to the axis of rotation (the *z*-axis). Contributions to the remanent magnetization come from grains with an easy axis of magnetization in the belts (rotational symmetry) limited as indicated (bold periphery) by θ_0 in case of incoherent reversal or $45^\circ - \psi_0$ in case of coherent reversal. These are the grains which at some point will have their easy axis of magnetization at angles close to 0 or 45° to the magnetizing field for incoherent and coherent reversal respectively. Demagnetization is carried out with the field applied along the *z*-axis, preserving the rotational symmetry around the *z*-axis.

A sample of crushed natural magnetite (SD3), probably slightly oxidized, was likewise prepared by distributing the magnetic material in a resin.

A sample of Pleistocene marine sediments (Y87) from the Fram Strait, Arctic Ocean, was dried out and cast into a resin to avoid disintegration during the experiment. Thermomagnetic analysis suggests that the magnetic mineral of interest for the demagnetization experiment is a cation-deficient spinel, which breaks down at temperatures around 350 °C.

Four samples of igneous rock were studied. Two samples, Dg1 and Dg17, represent a Pleistocene vesicular basalt from Dongshuiton, China. Thermomagnetic analysis typically revealed Curie points of 540–580 °C indicating low Ti titanomagnetite.

T97A and T54A are from a sill and a flood basalt respectively, both representing Triassic vulcanics from the Taimyr Peninsula in Arctic Russia. Reflected light microscopy reveals that the flood basalt (T97A) contains small skeletal grains of homogeneous titanomagnetite, attesting to rapid cooling of the rock. A Curie temperature of 430 °C supports these observations. The sill sample (T54A) contains larger titanomagnetite grains with exsolution lamellae of ilmenite, indicating deuteric oxidation. A dominant reversible Curie point of 580 °C is consistent with pure magnetite being the magnetic constituent in the grains.

For calculation of demagnetization curves, samples are assumed to be perfectly isotropic. Anisotropy of magnetic susceptibility (AMS), $\chi_{\max}/\chi_{\min}$, was less than 3 per cent for the igneous rock, about 5 per cent for the sediment, 9 per cent for the crushed magnetite sample and 5 and 1 per cent for the samples of γ-Fe_2O_3 and CrO_2 recording particles respectively, indicating that the error in this assumption is relatively minor.

Table 1. List of samples studied. The values of ARM and RRM used for the experiment are given relative to SIRM acquired in 4 T. For most samples the rotation speed for RRM acquisition was approximately 90 rotations per second (rps), but samples T54A and T97A were rotated at only 70 and 65 rps due to their weight and imperfect shape. For CrO_2, 63 rps was used to maximize RRM (Madsen 2003). See text for the definition of B_g.

Sample	Origin	SIRM (A m^{-1})	ARM (per cent)	RRM (per cent)	B_g (μT)
SR8	BASF γ-Fe_2O_3	4.16	5.25	4.02	128
CK4013	BASF CrO_2	139.19	0.51	0.06	−15
SD3	Crushed magnetite	5.91	0.31	1.15	330
Y87	Marine sediment	17.54	2.39	1.52	89
DG1	Vesicular basalt	872.11	2.19	1.78	34
DG17	Vesicular basalt	177.65	13.42	5.71	26
T97A	Flood basalt	93.64	5.49	0.35	9
T54A	Sill	350.85	1.66	0.39	38

Figs 4 and 5 display data from the two demagnetizations and suitable model predictions for the uniaxial demagnetization as calculated from the coercivity spectrum derived from demagnetization with tumbling. The magnitude of ARM and RRM as used for the

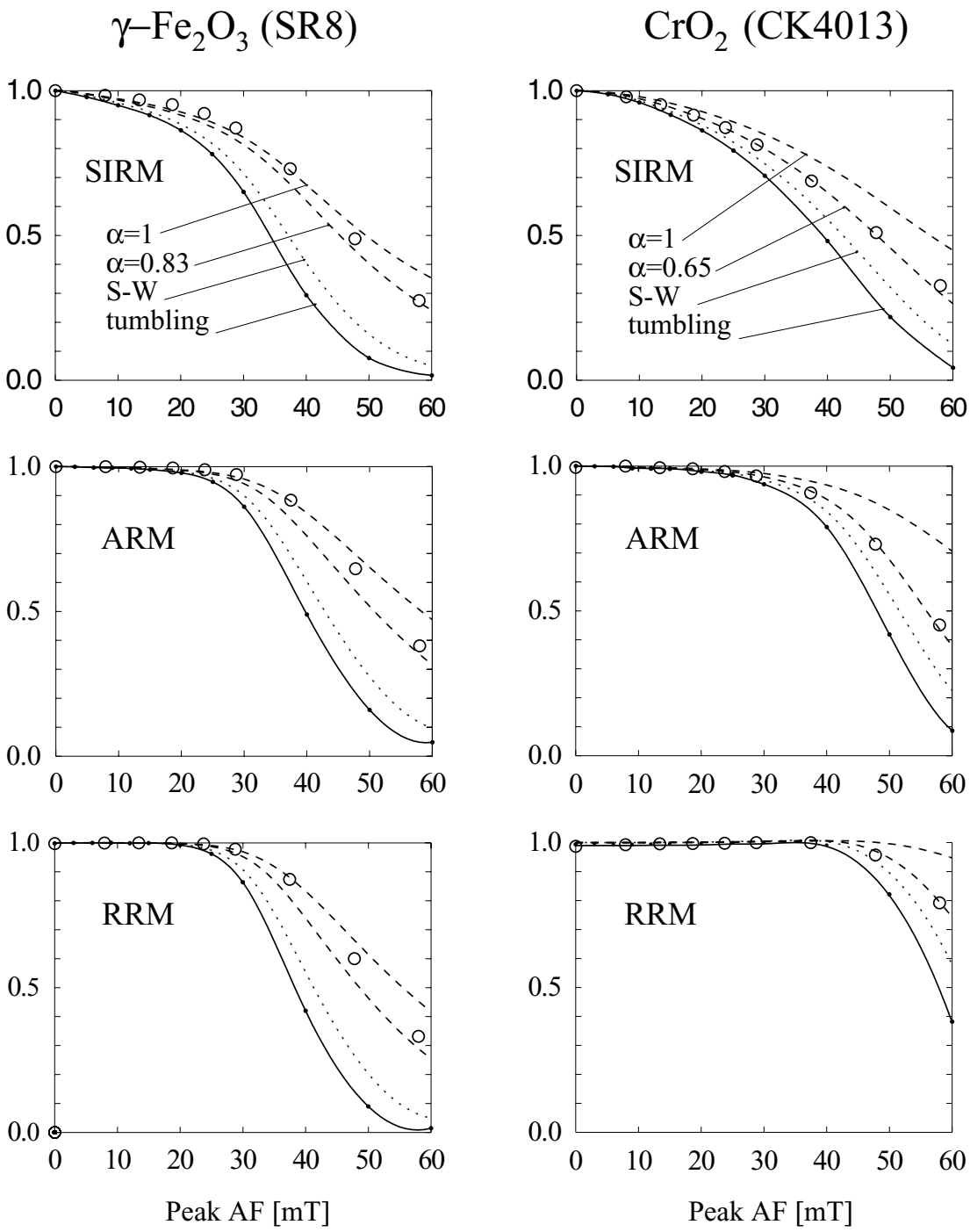

Figure 4. Demagnetization curves of SIRM, ARM and RRM for samples of (left) γ-Fe_2O_3 and (right) CrO_2 recording particles. Data from AF demagnetization with tumbling (full line with data points indicated) are used to calculate predictions for demagnetization with the AF applied only along the axis of remanence (dotted and dashed lines for models of coherent and incoherent reversal) which are compared with data (circles). Two separate curves are given for incoherent reversal in each diagram using α values of 0.83 and 1 for γ-Fe_2O_3 and 0.65 and 1 for CrO_2. For γ-Fe_2O_3 eq. (2) with $\alpha = 1$ models data well for low fields, while the value of α required for a good fit to data changes gradually towards 0.83 for higher fields. This result is in agreement with the conclusions from a previous study on the same particles (Madsen 2002). For CrO_2, a quite low α value of 0.65 provides the best fit to data.

demagnetization experiment is given relative to SIRM in Table 1. RRM relative to ARM is given in terms of the effective field, B_g, which can be considered to produce RRM. In most cases the values indicated differ slightly from those obtained from the RRM and ARM given in the table. This deviation arises because B_g was determined using the standards of Stephenson & Molyneux (1987).

DISCUSSION

Samples of recording particles

For the γ-Fe_2O_3 particles a previous study indicated that the angular dependence of the switching field is well described by relation

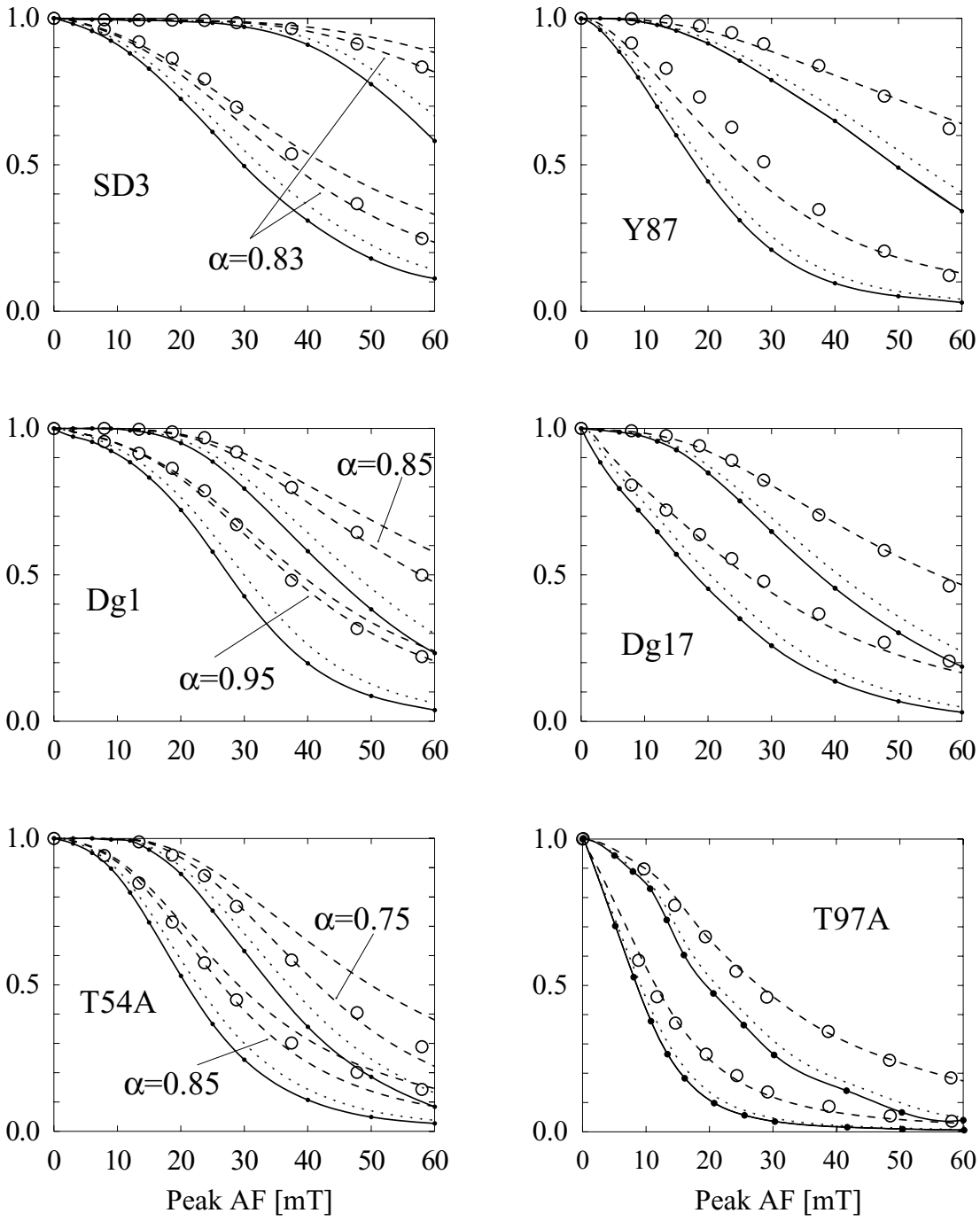

Figure 5. Demagnetization curves of ARM (lower curve family) and RRM (upper curve family) for the sample of crushed magnetite (SD3), the sediment sample (Y87) and the four natural rock samples (Dg1, Dg17, T97A, T54A). The use of full, dotted and dashed lines is as in Fig. 4. Values of α, when different from 1, are indicated.

(2), with α decreasing from about 1 to 0.83 for increasing particle coercivity (Madsen 2002). These results were derived from IRM measurements and are confirmed by the present demagnetization experiment carried out on SIRM. A good prediction for the intensity decrease in uniaxial demagnetization of the SIRM is obtained with $\alpha = 1$ for low fields, gradually changing towards $\alpha = 0.83$ as grains of higher coercivity are activated (Fig. 4). This trend is repeated for ARM and RRM. The coercivity spectra of ARM and RRM are almost identical and the variation of inferred α is also very similar, suggesting that ARM and RRM are carried by the same fraction of particles for this sample.

In contrast, RRM of the CrO_2 particles is a significantly harder remanence than ARM, which in turn is harder than SIRM (Fig. 4). Furthermore the magnitude of RRM relative to ARM is much smaller for CrO_2 than for γ-Fe_2O_3, as expressed by the magnitude of B_g (Table 1). The negative sign of B_g for CrO_2 reflects that the RRM of CrO_2 for unknown reasons is antiparallel to the rotation vector at high speeds (Madsen 2003) rather than parallel as expected and as

found for other materials investigated. The single-axis demagnetization results for the part of RRM and ARM demagnetized below 60 mT are both well modelled by relation (2) with $\alpha = 0.65$. This low value of α corresponds to a quite weak angular dependence of the switching field (Fig. 1). Alternatively, different switching modes could be present, α representing an averaged value lowered by a significant contribution from coherently switching grains. The specific remanent magnetization of the CrO_2 particles is similar to that of γ-Fe_2O_3, but the particles are about half the length, and magnetocrystalline anisotropy is more dominant, implying that coherent reversal is more likely for the CrO_2 than for the γ-Fe_2O_3 particles (Köster 1996).

Samples of crushed magnetite and natural rock

The chemical composition and crystal structure of the γ-Fe_2O_3 recording particles is quite similar to that of the natural oxidized magnetite or titanomagnetite present in the igneous rock samples. In contrast to the natural samples, however, the synthetic γ-Fe_2O_3 sample contains only SD grains with a narrow distribution of grain sizes, which are expected to be very good RRM and ARM carriers in accordance with the use, for example by environmental magnetists, of ARM/SIRM as a grain size indicator. In addition to the contribution from SD grains, SIRM of natural samples also includes contributions from MD grains and from high-coercivity grains which are not activated by the field used to induce ARM and RRM. For this reason it is surprising that the magnitude of ARM and RRM relative to SIRM is not much larger for synthetic γ-Fe_2O_3 than for natural samples (Table 1). The data indicate that the ratio ARM/SIRM depends on more variables and should be used with caution as a grain size indicator.

As for the synthetic samples, single-axis demagnetization results of the natural samples and the crushed magnetite differ more from those of tumbling than expected from the model of coherent reversal. The lag is much better accounted for by assuming relation (2) to be valid for the switching field with α varying from 0.75 to 1. Higher values of α seem to apply to samples of magnetically softer remanences. A similar tendency is observed for individual samples in that ARM, which is a softer remanence than RRM for all samples, is modelled with a higher α than RRM. For Y87, Dg17 and T97A, which are the samples with the softest ARM, the angular dependence of the switching field seems to be stronger than that modelled with $\alpha = 1$.

The slightly different models applying to RRM and ARM could be an artefact arising if the acquisition of RRM is not similar to that of ARM as assumed when calculating the curves, but is enhanced relative to ARM for grains with easy axes at low angles to the field. However, the difference, if any, suggested by the data of Stephenson & Potter (1987) is the opposite. Furthermore no significant difference is observed for the data from γ-Fe_2O_3 recording particles, which is the only sample for which the coercivity spectrum supports the possibility that RRM and ARM are due to the same fraction of grains.

The natural samples represent a much broader variety of grain size and chemical composition and α is more likely to be an average value for different grains of similar coercivity. Higher values of α for ARM than for RRM and for samples of softer remanence compared with samples of harder remanence may result from larger relative contributions from PSD or MD grains (Mahon & Stephenson 1997). This would imply that a stronger angular dependence seems to be associated with domain-wall motion in MD grains than with switching for SD grains. A minor occurrence of grains with coherent switching cannot be ruled out, as low values of α could be due to a mixture a of grains, some described by relation (2) with higher α, some reversing coherently.

IMPLICATIONS FOR DEMAGNETIZATION METHODS

Considering Fig. 3, it is clear that a better coverage of directions is associated with a small ψ_h in the case of coherent reversal than a similar θ_h for incoherent reversal. This is the main reason why a switching field angular dependence of the type described by relation (2) will have more severe implications for magnetization and demagnetization than that of coherent reversal. The stronger effect related to (2) compared with coherent reversal, even for small α, is illustrated by the longer 'tails' of remanence surviving demagnetization to fields in excess of the coercivity (Fig. 2). Although uniaxial demagnetization is not used for uncovering NRM directions it is sometimes carried out for other palaeomagnetic purposes, for example the Lowrie–Fuller test. Furthermore it may be noted that the curves given for demagnetization of SIRM correspond to acquisition of IRM, which is commonly used to obtain coercivity spectra of SIRM.

When applying the field along more than one axis, as is done for palaeomagnetic demagnetization purposes, the tails of the demagnetization curves will be reduced. Still, static three-axis demagnetization is somewhat less efficient than demagnetization with tumbling and will give rise to some mixing of remanence components residing in different coercivity fractions (McFadden 1981). The present study has focused particularly on RRM, which may be considered a special type of gyromagnetic remanent magnetization (GRM). This remanence may also form during static 'demagnetization' if the sample is not perfectly isotropic (Stephenson 1980), giving rise to spurious components of magnetization. The implications of relation (2) to GRM formation in three-axis demagnetization are discussed below.

Consider a sample of uniaxial anisotropy due to a preferred direction of the easy magnetization axes of the magnetic grains. If an alternating field is applied at an angle to the axis of anisotropy, GRM is formed perpendicular to the field and to the axis of anisotropy. Based on this observation Dankers & Zijderveld (1981) suggested a method for eliminating GRM from data obtained by three-axis demagnetization. For each new field strength, the AF is first applied along the x-, y- and z-axes (AF_x, AF_y and AF_z). Then each component of remanence is measured after repeated application of the field in the corresponding direction. However, due to the angular dependence of switching field, AF_x, AF_y and AF_z will not activate the same grains unless the field is saturating. Hence, GRM resulting from application of an AF in one direction will not necessarily be removed by a perpendicular AF of the same peak field strength. GRM resides in grains that are at least as stable as the carriers of NRM, so the case of non-saturating fields must be considered since saturating fields would have removed the NRM completely.

Assuming an incoherent reversal mode, the first grains activated by the AF are those with easy axes in the vicinity of the x-, y- and z-axes. For a peak AF sufficiently small compared with the minimum switching field, no grain will be activated by more than one of AF_x, AF_y and AF_z (Fig. 6a). The magnitude of GRM to a first approximation is proportional to $\sin(2v)$, v being the angle between the AF axis and the axis of anisotropy (Stephenson 1981). In this

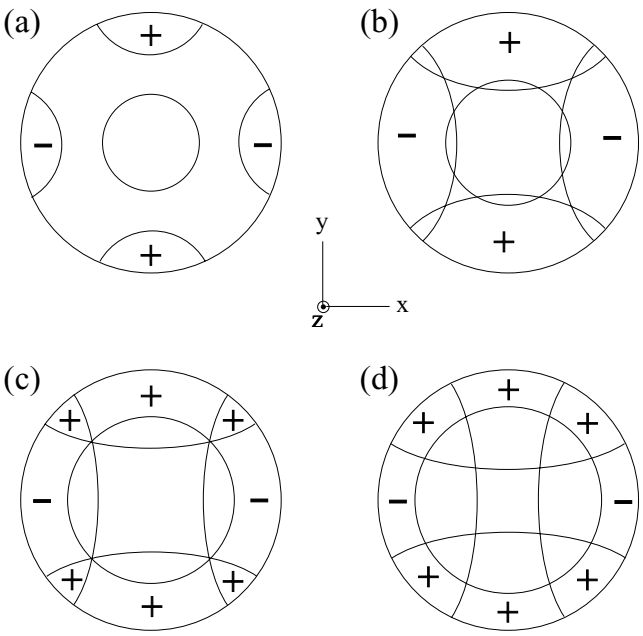

Figure 6. GRM formation in three-axis 'demagnetization' of an anisotropic sample of identical magnetic grains. The alternating field is applied along the *x*-, *y*- and *z*-axis. With the axis of alignment in the *x*–*y* plane, application of AF_x and AF_y gives rise to GRM components parallel and antiparallel to the *z*-axis, while no GRM arise from application of AF_z. The order of field application before measuring the *z*-component of remanence is AF_x, AF_y and AF_z. (a) For small peak AF, only grains with an easy axis at low angles to the field, i.e. either the *x*-, *y*- or *z*-axis are activated by the field. The GRM contributions from each zone cancel out. (b), (c), (d) For higher peak AF the zones of activation by AF_x, AF_y and AF_z overlap. Grains activated by more than one of the fields will contribute to the GRM direction associated with the direction of the last field applied. Grains eventually activated by AF_z do not contribute to GRM.

case GRM contributions from individual circle areas cancel each other out. As the peak AF is increased, the activation zones of AF_x, AF_y and AF_z eventually overlap and some grains will be activated first by two (Figs 6b and c) and eventually all three (Fig. 6d) of AF_x, AF_y and AF_z. This destroys the balance between GRM of individual areas and a net GRM may result.

Consider a simple case where the axis of anisotropy is in the *x*–*y* plane. Application of AF_x and AF_y will result in antiparallel GRM components in the *z*-direction. In the case of no overlap (Fig. 6a), these components will be of the same size and opposite sign and will cancel out. When overlap occurs (Figs 6b, c and d), a net GRM in the direction determined by the last field applied before AF_z (i.e. AF_y) may result. Only some of it will be demagnetized by AF_z before measuring the *z*-component. Note that NRM carried by the same fraction of grains will be eliminated at step (c) (all grains activated by at least one of AF_x, AF_y and AF_z), while GRM is not completely eliminated until the field reaches saturation (all grains activated by each of AF_x, AF_y and AF_z).

Theoretically this implies that the last remanence to be removed is a pure GRM component with a direction determined solely by the geometry of applied fields and anisotropy axes, i.e. without any relation to NRM. Since the GRM contribution to remanence is eventually eliminated using this method, a final contracting remanence vector in the Zijderfeld diagram is not a guarantee that GRM is not influencing the inferred NRM direction. In fact, the final component defined by the data could be partly or totally controlled by GRM. For natural samples possessing a range of coercivities, GRM is generally associated with a spectrum of higher coercivities than NRM and the above argument remains valid.

CONCLUSIONS

Demagnetization curves for ARM and RRM obtained by AF application along the axis of remanence only lag behind the curves obtained with tumbling of the sample in the AF. This lag was determined for synthetic samples of recording particles and crushed magnetite as well as for natural rocks, and related to models of the angular dependence of the switching field, leading to the following conclusions:

(1) Data were not in accordance with the model for coherent reversal, but were generally modelled well assuming an angular dependence for the switching field given by $H_r(\theta) = H_r(0)/\sqrt{1-\alpha \sin^2\theta}$, with $0.75 < \alpha < 1$. This relation has been suggested to describe incoherent reversal, but domain wall movements may give rise to similar results.

(2) For synthetic samples, SIRM, ARM and RRM were all modelled with the same values of α, reflecting the homogeneity of the grains of these samples. For CrO_2, data indicated a quite weak angular dependence of switching field ($\alpha \sim 0.65$).

(3) For natural samples, lower values of α (i.e. weaker angular dependence), tend to be associated with higher coercivities as for the γ-Fe_2O_3 recording particles. Since natural samples contain a variety of grains the value of α is an average which does not necessarily describe $H_r(\theta)$ for one type of grain. A larger α associated with lower coercivities could result from larger contributions from MD grains and a lower α associated with higher coercivities may be attributed to minor contributions from coherently switching SD grains

(4) Assuming an angular dependence of the switching field corresponding to incoherent reversal, the influence of GRM on three-axis AF demagnetization data cannot be eliminated completely by the procedure of Dankers & Zijderveld (1981).

(5) The ratio ARM/SIRM, often used as a grain size indicator, cannot be trusted to reflect grain size when more than one lithology is considered

ACKNOWLEDGMENTS

I thank Alan Stephenson, Harald Walderhaug and Reidar Løvlie for supplying the recording particles, the crushed magnetite and the sediment and rock samples. The valuable and constructive comments of Harald Walderhaug, Reidar Løvlie, David Potter, Ramon Egli and E. Appel improved the manuscript significantly. The B_g measurements were carried out during a brief visit to the University of Newcastle. The work presented in this paper was carried out while the author was in receipt of a PhD scholarship from the Danish Research Council.

REFERENCES

Aharoni, A., 1986. Angular dependence of nucleation field in magnetic recording particles, *IEEE Trans. Magn.,* **MAG-22,** 149–150.

Dankers, P.H.M. & Zijderveld, J.D.A., 1981. Alternating field demagnetization of rocks, and the problem of gyromagnetic remanence, *Earth planet. Sci. Lett.,* **53,** 89–92.

Enkin, R. & Williams, W., 1994. Three-dimensional micromagnetic analysis of stability in fine magnetic grains, *J. geophys. Res.,* **99,** 611–618.

Frei, E.H., Shtrikman, S. & Treves, D., 1957. Critical size and nucleation field of ideal ferromagnetic particles, *Phys. Rev.,* **106,** 446–455.

Hu, S., Appel, E., Hoffmann, V., Schmal, W.W. & Wang, S., 1998. Gyromagnetic remanence acquired by greigite during static three-axis alternating field demagnetization, *Geophys. J. Int.,* **134,** 831–842.

Jacobs, I.S. & Bean, C.P., 1955. An approach to elongated fine-particle magnets, *Phys. Rev.,* **100,** 1060–1067.

Köster, E., 1996. Particulate media, in *Magnetic Recording Technology,* pp. 3.1–3.74, eds Mee, C.D. & Daniel, E.D., McGraw-Hill, New York.

Madsen, K.N., 2002. Angular dependence of switching field measured on maghemite recoding particles, *J. Magn. Magn. Mater.,* **241,** 220–227.

Madsen, K.N., 2003. A reversed gyromagnetic effect in chromium dioxide particles, *J. Magn. Magn. Mater.,* **260,** 131–140.

Mahon, S.W. & Stephenson, A., 1997. Rotational remanent magnetization (RRM), and its high temporal and thermal stability, *Geophys. J. Int.,* **130,** 383–389.

McFadden, P.L., 1981. A theoretical investigation of the effect of individual grain anisotropy in alternating field demagnetization, *Geophys. J. R. astr. Soc.,* **67,** 35–51.

Moon, T. & Merrill, R.T., 1988. Single-domain theory of remanent magnetization, *J. Geophys. Res.,* **93,** 9202–9210, 1988.

Potter, D.K. & Stephenson, A., 1986. The detection of fine particles of magnetite using anhysteretic and rotational remanent magnetizations, *Geophys. J. R. astr. Soc.,* **87,** 569–582.

Stephenson, A., 1980. A gyroremanent magnetisation in anisotropic magnetic material, *Nature,* **284,** 49–51.

Stephenson, A., 1981. Gyromagnetic remanence and anisotropy in single-domain particles, rocks, and magnetic recording tape, *Phil. Mag. B,* **44,** 635–664.

Stephenson, A., 1983. Changes in direction of the remanence of rocks produced by stationary alternating field demagnetization, *Geophys. J. R. astr. Soc.,* **73,** 213–239.

Stephenson, A. & Molyneux, L., 1987. The rapid determination of rotational remanent magnetization and the effective field which produces it, *Geophys. J. R. astr. Soc.,* **90,** 467–471, 1987.

Stephenson, A. & Potter, D.K., 1987. Gyroremanent magnetizations in dilute anisotropic dispersions of gamma ferric oxide particles from magnetic recording tape, *IEEE Trans. Magn.,* **MAG-23,** 3820–3830.

Stoner, E.C. & Wohlfarth, E.P., 1948. A mechanism of magnetic hysteresis in heterogeneous alloys, *Phil. Trans. R. Soc. Lond.* A, **240,** 599–642.

APPENDIX

The calculation of $I_{H_c}(\mathrm{H})$ for an isotropic sample of one coercivity $H_c = H_r(0)$ is given in units of H_c, i.e. using reduced fields $h = H/H_c$.

Incoherent reversal

For incoherent reversal modes the switching field h is increasing with increasing angle between the field and the easy axis of the grain according to:

$$h = \frac{1}{\sqrt{1-\alpha\sin^2\theta}}. \tag{3}$$

In the case of ARM, a magnetizing AF of peak strength h_0 is applied in the x–y plane, and the grains contributing to remanence are those with easy axis in the belt sketched in Fig. 3(a). Saturation of remanence, i.e. $\theta_0 = \pi/2$ or $\omega_0 = 0$, requires a peak AF of strength $h_0 \geq 1/\sqrt{1-\alpha}$. For $h_0 < 1/\sqrt{1-\alpha}$ the limiting polar angle $\omega_0 = \frac{\pi}{2} - \theta_0$ is derived from:

$$h_0 = \frac{1}{\sqrt{1-\alpha\sin^2(\frac{\pi}{2}-\omega_0)}} \iff$$

$$\omega_0 = \frac{\pi}{2} - \arcsin\left(\sqrt{\frac{1}{\alpha}\left(1-\frac{1}{h_0^2}\right)}\right) \tag{4}$$

$$= \arccos\left(\sqrt{\frac{1}{\alpha}\left(1-\frac{1}{h_0^2}\right)}\right). \tag{5}$$

Decrease of remanence by demagnetization is initiated as the AF applied in the z-direction exceeds a peak value h_1 given by

$$h_1 = \frac{1}{\sqrt{1-\alpha\sin^2\omega_0}}. \tag{6}$$

Demagnetization is completed for $h_2 = 1/\sqrt{1-\alpha}$. For $h_1 < h < h_2$ the AF of peak strength h will demagnetize grains with an easy axis of polar angle up to $\theta_h > \omega_0$, where

$$\theta_h = \arcsin\left(\sqrt{\frac{1}{\alpha}\left(1-\frac{1}{h^2}\right)}\right). \tag{7}$$

Following Stephenson (1983), the contribution to ARM from grains of polar angle ω is taken as proportional to $\cos^2\omega$ Stephenson (1983). A factor $2\pi\,\sin\omega$ arises from integrating over the azimuthal angle, so the demagnetization curve is given by

$$\begin{aligned}\frac{I_{\mathrm{ARM}}(h)}{I_{\mathrm{ARM}}(0)} &= \frac{\int_{\theta_h}^{\pi/2}\cos^2\omega\sin\omega\,d\omega}{\int_{\omega_0}^{\pi/2}\cos^2\omega\sin\omega\,d\omega}\\ &= \frac{\cos^3\theta_h}{\cos^3\theta_0}\\ &= \left(\frac{1}{\alpha}\left(1-\frac{1}{h_0^2}\right)\right)^{-3/2}\\ &\quad\times\cos^3\left(\arcsin\sqrt{\frac{1}{\alpha}\left(1-\frac{1}{h^2}\right)}\right).\end{aligned} \tag{8}$$

In the case of saturation ($\omega_0 = 0$), the intensity decrease starts from $h_1 = 1$ and decreases to zero for $h_2 = 1/\sqrt{1-\alpha}$. For $1 < h < h_2$ relation (8) reduces to

$$\frac{I_{\mathrm{ARM}}(h)}{I_{\mathrm{ARM}}(0)} = \cos^3\left(\arcsin\sqrt{\frac{1}{\alpha}\left(1-\frac{1}{h^2}\right)}\right). \tag{9}$$

For IRM the magnetizing field h_0 is applied along the axis of remanence and

$$\omega_0 = \theta_0 = \arcsin\left(\sqrt{\frac{1}{\alpha}\left(1-\frac{1}{h_0^2}\right)}\right). \tag{10}$$

By demagnetization along the same axis, the intensity starts decreasing when the peak AF reaches $h = 1$ and will be completely removed as the peak AF exceeds h_0. For $1 < h < h_0$, contributions to remanence from grains associated with angles up to θ_h will be eliminated, where

$$\theta_h = \arcsin\left(\sqrt{\frac{1}{\alpha}\left(1-\frac{1}{h^2}\right)}\right), \tag{11}$$

and the intensity decrease is given by

$$\begin{aligned}\frac{I_{\mathrm{IRM}}(h)}{I_{\mathrm{IRM}}(0)} &= \frac{\int_{\theta_h}^{\theta_0}\cos\omega\sin\omega\,d\omega}{\int_{0}^{\theta_0}\cos\omega\sin\omega\,d\omega}\\ &= \frac{\sin^2\theta_0-\sin^2\theta_h}{\sin^2\theta_0}\\ &= \frac{1/h^2-1/h_0^2}{1-(1/h_0^2)}.\end{aligned} \tag{12}$$

For $h_0 > 1/\sqrt{1-\alpha}$ the remanence is saturated (SIRM). In this case the intensity decrease is obtained from (12) by substituting $1/h_0^2 = 1-\alpha$:

$$\frac{I_{SIRM}(h)}{I_{SIRM}(0)} = 1 - \frac{1}{\alpha}\left(1 - \frac{1}{h^2}\right). \tag{13}$$

Coherent reversal

For coherent reversal the switching field is minimum for $\theta = \pi/4$ and increases symmetrically for angles $\pi/4 \pm \psi$ between field and the easy axis of the grain (Fig. 3). The analytical expression for $\psi(h)$ as given by Stephenson (1983) is:

$$\psi = \frac{\pi}{4} - \frac{1}{2}\arcsin\left[\frac{8}{3\sqrt{3}}\frac{1}{h^2}\left(1 - \frac{1}{4}h^2\right)^{3/2}\right]. \tag{14}$$

Due to the rotation of the sample in the case of ARM, a peak AF h_0 magnetizes grains in a belt limited by polar angle $\frac{\pi}{4} - \psi_0$, $\psi_0 = \psi(h_0)$. Demagnetization is effective from $h = 1$ and is completed for $h = 2$ in the unsaturated case. For $1 < h < h_0$ the intensity decrease of ARM is given by

$$\begin{aligned}\frac{I_{\mathrm{ARM}}(h)}{I_{\mathrm{ARM}}(0)} &= \left[\left(\int_{\pi/4-\psi_0}^{\pi/2} \cos^2\omega \sin\omega\, d\omega\right) - \left(\int_{\pi/4-\psi_h}^{\pi/4+\psi_h} \cos^2\omega \sin\omega\, d\omega\right)\right] \times \left(\int_{\pi/4-\psi_0}^{\pi/2} \cos^2\omega \sin\omega\, d\omega\right)^{-1} \\ &= 1 - \frac{\cos^3(\pi/4-\psi_h) - \cos^3(\pi/4+\psi_h)}{\cos^3(\pi/4-\psi_0)},\end{aligned} \tag{15}$$

with $\psi_h = \psi(h)$ given by (14). For $h_0 < h < 2$ the intensity decrease of ARM is given by

$$\begin{aligned}\frac{I_{\mathrm{ARM}}(h)}{I_{\mathrm{ARM}}(0)} &= \frac{\int_{\pi/4+\psi_h}^{\pi/2} \cos^2\omega \sin\omega\, d\omega}{\int_{\pi/4-\psi_0}^{\pi/2} \cos^2\omega \sin\omega\, d\omega} \\ &= \frac{\cos^3(\pi/4+\psi_h)}{\cos^3(\pi/4-\psi_0)}.\end{aligned} \tag{16}$$

For $h_0 \geq 2$ the remanence is saturated, i.e. $\psi_0 = \pi/4$ and for $1 < h < 2$ the expression reduces to

$$\frac{I_{\mathrm{ARM}}(h)}{I_{\mathrm{ARM}}(0)} = 1 - [\cos^3(\pi/4-\psi_h) - \cos^3(\pi/4+\psi_h)]. \tag{17}$$

Considering IRM and SIRM, the magnetizing and demagnetizing field are both applied along the z-axis of Fig. 3. Demagnetization is effective from $h = 1$ and is completed for $h = h_0$. For $1 < h < h_0$ the intensity decrease of IRM is given by

$$\begin{aligned}\frac{I_{\mathrm{IRM}}(h)}{I_{\mathrm{IRM}}(0)} &= \left[\left(\int_{\pi/4-\psi_0}^{\pi/4+\psi_0} \cos\omega \sin\omega\, d\omega\right) - \left(\int_{\pi/4-\psi_h}^{\pi/4+\psi_h} \cos\omega \sin\omega\, d\omega\right)\right] \times \left(\int_{\pi/4-\psi_0}^{\pi/4+\psi_0} \cos\omega \sin\omega\, d\omega\right)^{-1} \\ &= 1 - \frac{\cos^2(\pi/4-\psi_h) - \cos^2(\pi/4+\psi_h)}{\cos^2(\pi/4-\psi_0) - \cos^2(\pi/4+\psi_0)},\end{aligned} \tag{18}$$

with ψ_0 and ψ_h given by (14). For $h_0 \geq 2$ the remanence is saturated, i.e. $\psi_0 = \pi/4$ and for $1 < h < 2$ expression (18) reduces to

$$\frac{I_{\mathrm{IRM}}(h)}{I_{\mathrm{IRM}}(0)} = 1 - (\cos^2(\pi/4-\psi_h) - \cos^2(\pi/4+\psi_h)). \tag{19}$$